

Bounds on boosted dark matter from direct detection: The role of energy-dependent cross sections

Debjyoti Bardhan,^{1,*} Supritha Bhowmick,^{1,†} Diptimoy Ghosh,^{1,‡} Atanu Guha,^{1,2} and Divya Sachdeva^{3,§}

¹*Department of Physics, Indian Institute of Science Education and Research Pune, India*

²*Department of Physics, Chungnam National University, South Korea*[¶]

³*Laboratoire de Physique Théorique et Hautes Énergies (LPTHE),*

UMR 7589 CNRS and Sorbonne Université, 4 Place Jussieu, F-75252, Paris, France

The recoil threshold of Direct Detection (DD) experiments limits the mass range of Dark Matter (DM) particles that can be detected, with most DD experiments being blind to sub-MeV DM particles. However, these light DM particles can be boosted to very high energies via collisions with energetic Cosmic Ray electrons. This allows Dark Matter particles to induce detectable recoil in the target of Direct Detection experiments. We derive constraints on scattering cross section of DM and electron, using XENONnT and SUPER-KAMIOKANDE data. Vector and scalar mediators are considered, in the heavy and light regimes. We discuss the importance of including energy dependent cross sections (due to specific Lorentz structure of the vertex) in our analysis, and show that the bounds can be significantly different than the results obtained assuming constant energy-independent cross-section, often assumed in the literature for simplicity. Our bounds are also compared with other astrophysical and cosmological constraints.

I. INTRODUCTION

One of the strongest indicators of Physics Beyond the Standard Model (BSM) is Dark Matter (DM). Its existence can be inferred from diverse observations like galaxy rotation curves, cosmic microwave background radiation (CMBR) and gravitational lensing [1–3]. Expectedly, massive experimental and observational efforts have been undertaken to understand its composition and interactions. Moreover, details of structure formation constrain the type of DM and we know that it is only cold dark matter (CDM) which fits all the evidence. However, these observations remain mute about the exact composition of DM and the interactions it has with itself and SM particles besides gravitation.

Experiments aimed at investigating particle nature of DM are divided into two categories - indirect detection and direct detection (DD) experiments. Indirect detection experiments [4] focus on the study of signatures of the creation or annihilation of DM. Annihilation or decay of DM might produce excess photons in a certain mass window over the SM background, from which the mass of the DM can be inferred. The obvious challenge in this methodology is the very low signal production, which can be difficult to distinguish over the SM background, not to mention the difficulty in modelling the SM photon background in the first place. The basic idea of DD experiments is that DM particles impinge on a detector and transfer a part of their kinetic energy to the target. The rate of such scattering events in a certain recoil energy bin yields DM interaction cross section

bounds. Despite intense efforts on DD experiments all around the globe, the search for DM has been fruitless. Some experiments have seen tantalising hints [5, 6], but nothing definitive has come of those [7].

The average velocity of DM particles in the solar neighbourhood is $v/c \sim 10^{-3}$ which limits the energy to be deposited in a detector. Therefore, scattering in the direct detection is assumed to be non-relativistic (NR). With detectors like XENON1T that has a minimum electronic recoil energy threshold of $\sim \mathcal{O}(1 \text{ keV})$, the smallest accessible DM mass (m_χ) is $m_\chi \sim \mathcal{O}(1 \text{ MeV})$. For SUPER-KAMIOKANDE (SUPER-K), which has a minimum recoil energy threshold of $\sim \mathcal{O}(1 \text{ MeV})$, the smallest accessible DM mass is $\sim \mathcal{O}(1 \text{ GeV})$ ¹. These detectors cannot access lighter DM particles in this scenario.

However, as DM particles interact with cosmic rays (CR), it is inevitable that some DM particles will be boosted due to scattering by energetic CR particles [11–23]. In this study we focus on boosting of DM particles by CR electrons only; for boosting of DM by CR nucleons and neutrinos, refer to [11, 13, 23–26]. Since boosted particles can carry large amounts of kinetic energy, even very light DM particles can deposit a recoil energy $E_R > E_c$ in a detector, where E_c is the lower detector threshold. Thus, direct detection detectors as well as neutrino experiments can become sensitive to very low mass DM. However, the sensitivity at lower DM masses is achieved at larger cross sections because the upscattered subcomponent flux is substantially lower than the galactic DM population. Note that CRe is one of sources of boosting DM particles among others, such as blazars [27, 28], helium nuclei [11], Diffuse Supernova

* debjyoti.bardhan@acads.iiserpune.ac.in

† supritha.bhowmick@students.iiserpune.ac.in

‡ diptimoy.ghosh@iiserpune.ac.in

§ dsachdeva@lpthe.jussieu.fr

¶ atanu@cnu.ac.kr

¹ An exception to this occurs in fermionic DM absorption models, for which XENON-1T can probe DM masses down to $\sim \mathcal{O}(10 \text{ keV})$ and SUPER-K can probe masses of $\sim \mathcal{O}(1 \text{ MeV})$ [8–10]

Neutrino Background (DSNB) [18–22] and non-galactic contributions to DM flux [29].

In most of the existing literature, DM interaction cross-sections have largely been taken to be independent of the DM energy. This is a good approximation when i) the DM is non-relativistic and ii) the DM mediator is heavy. These assumptions will not hold when : i) DM becomes relativistic upon getting upscattered by energetic particles, and ii) mediator is light. The DM boost phenomena introduces non-trivial energy dependences for both heavy and light dark mediator ². The exact energy dependence is operator dependent. The importance of energy-dependent scattering has been recently highlighted in a few works [15, 24, 30–32], where it was found that the resulting limits are orders of magnitude different than those derived under the assumption of a constant cross section.

In this paper we consider the direct detection of DM particles, boosted by Cosmic Ray electron (CRe) via recoil of electrons in detectors in specific models of fermionic DM interactions. The remainder of this work is organized as follows. In Sec. II we discuss how to obtain the DM flux and the event rate from an upscattered DM. Specifically, we show the effects of energy

dependence of the cross-section on the flux, as induced by the Lorentz structure of the operator, and compare it to the boosted constant cross-section case. In Sec. III we consider specific operators. Explicit connections of these operators to well-motivated models of DM are also drawn. Sec. IV provides the results in the cross-section mass plane from SUPER-K and XENONnT, along with a discussion on cosmological constraints from BBN as well as collider constraints. We summarise and conclude in Sec.V.

II. BOOSTED DARK MATTER FLUX AND EVENT RATE

The DM particles contained in the DM halo within the Milky Way galaxy follow a curtailed Maxwell-Boltzmann velocity distribution, with the average velocity at about $v \sim 10^{-3}$ (with $c = 1$). It is inevitable that the energetic Cosmic Ray electrons will interact with non-relativistic DM particles and may provide them a large boost to velocities $v \gg 10^{-3}$. CR electron flux ($F(T_e)$) can be described by certain parameterization of the local interstellar spectrum [33] given as

$$F(T_e) = \begin{cases} \frac{1.799 \times 10^{44} T_e^{-12.061}}{1 + 2.762 \times 10^{36} T_e^{-9.269} + 3.853 \times 10^{40} T_e^{-10.697}} & \text{if } T_e < 6880 \text{ MeV} \\ 3.259 \times 10^{10} T_e^{-3.505} + 3.204 \times 10^5 T_e^{-2.620} & \text{if } T_e \geq 6880 \text{ MeV} \end{cases} \quad (1)$$

where the unit of $F(T_e)$ is given in $(\text{m}^2 \text{ s sr MeV})^{-1}$ and the kinetic energy of the CR electrons (T_e) is in MeV. The above fit is consistent with Fermi-LAT [34–37], AMS-02 [38], PAMELA [39, 40], and Voyager [41, 42] local interstellar spectrum data, to within an accuracy of 5 % .

For a CR electron (CRe) hitting a DM particle, we have

$$T_\chi^{\text{max}} = \frac{T_e^2 + 2m_e T_e}{T_e + (m_e + m_\chi)^2 / (2m_\chi)} \quad (2)$$

$$T_\chi = T_\chi^{\text{max}} \frac{1 - \cos \theta}{2} \quad (3)$$

where $T_\chi(T_e)$ is the kinetic energy of the DM particle (CRe), $m_\chi(m_e)$ is the mass of the DM particle (CRe) and θ is the scattering angle in the centre of momentum frame.

The differential flux of the Boosted DM (BDM) is

then given by

$$\left(\frac{d\Phi_\chi}{dT_\chi} \right)_e = D_{\text{eff}} \times \frac{\rho_\chi^{\text{local}}}{m_\chi} \int_{T_e^{\text{min}}(T_\chi)}^{\infty} dT_e \frac{d\Phi_e}{dT_e} \frac{d\sigma_{\chi e}}{dT_\chi} \quad (4)$$

where $\Phi_\chi(\Phi_e)$ is the DM (CRe) flux, ρ_χ^{local} is the local DM density, $\sigma_{\chi e}$ is the DM-CRe interaction cross-section, D_{eff} ³ is the line-of-sight effective distance (taken to be 1 kpc), and T_e^{min} is the minimum kinetic energy CRe must possess to boost the DM particle to energy T_χ , given by :

$$T_e^{\text{min}} = \left(\frac{T_\chi}{2} - m_e \right) \left[1 \pm \sqrt{1 + \frac{2T_\chi (m_e + m_\chi)^2}{m_\chi (2m_e - T_\chi)^2}} \right] \quad (5)$$

with + and – applicable for $T_\chi > 2m_e$ and $T_\chi < 2m_e$ respectively.

² The mediator is charged under both the SM electroweak group, as well as the DM gauge group, allowing it to couple SM electrons to the DM particles

³ We need to consider all possible line segments along the line of sight, along which the DM particles are boosted after the interaction with CRe. D_{eff} is the effective distance out to which all CRe have to be taken into account

Of course,

$$\frac{d\sigma_{\chi e}}{dT_\chi} = \frac{|\mathcal{M}|^2}{16\pi s_{\text{CR}}} \frac{1}{T_\chi^{\text{max}}} \quad (6)$$

where \mathcal{M} is the interaction matrix element and s_{CR} is the centre of momentum energy for the CRe-DM collision, given by :

$$s_{\text{CR}} = (m_\chi + m_e)^2 + 2m_\chi T_e \quad (7)$$

Under the energy independent approximation for the cross section, the differential cross section would simply be :

$$\frac{d\sigma_{\chi e}}{dT_\chi} = \frac{\bar{\sigma}_{e\chi}}{T_\chi^{\text{max}}} \quad (8)$$

We define the following quantities :

$$\mathbb{M}^2 = \frac{16g_e^2 g_\chi^2 m_e^2 m_\chi^2}{(q_{\text{ref}}^2 - m_i^2)^2} \quad (9)$$

$$\bar{\sigma}_{e\chi} = \frac{\mu_{\chi e}^2}{16\pi m_e^2 m_\chi^2} \mathbb{M}^2 \quad (10)$$

where $q_{\text{ref}} = \alpha m_e$ is the reference momentum transferred. Here, g_χ (g_e) is the coupling constant of the dark mediator to the DM particle (electron), m_i is the mass of the dark mediator ($i = A', \phi$ for vector, scalar mediator) and $\mu_{e\chi}$ is the reduced mass of the DM-electron system.

The differential cross-section is given by

$$\frac{d\sigma_{\chi e}}{dE_R} = \frac{|\mathcal{M}|^2}{16\pi s_\chi} \frac{1}{E_R^{\text{max}}} \quad (11)$$

where s_χ is centre of momentum energy for the DM-target electron collision which can be obtained from Eqn. (7) under the substitution : $m_\chi \leftrightarrow m_e$ and $T_e \rightarrow T_\chi$. E_R^{max} is the maximum possible recoil in the detector, that can be imparted by a DM particle with kinetic energy T_χ , and can be obtained from Eqn. (2) with the appropriate substitutions mentioned before.

We can now define a form factor

$$F_{\text{DM}}^2(q^2) = |\mathcal{M}|^2 / \mathbb{M}^2 \quad (12)$$

This factor contains the energy dependence arising in the differential cross section $d\sigma_{\chi e}/dT_\chi$ due to CRe boosting the DM particles and the Lorentz structure of the interaction. The explicit form of F_{DM} depends on the model of DM and mediator considered.

A similar form factor, F_{rec} , contains energy dependence in the differential cross section $d\sigma_{\chi e}/dE_R$ arising due to interaction of relativistic DM particles with the electrons in the detector, and can be obtained from the form factor F_{DM} of Eqn. 12 by making the substitutions : $m_e \leftrightarrow m_\chi$, $T_\chi \rightarrow E_R$ and $T_e \rightarrow T_\chi$.

Hence the differential cross sections, $d\sigma_{\chi e}/dT_\chi$ and $d\sigma_{\chi e}/dE_R$, relevant in the DM-CRe scattering and DM scattering at the detector end respectively, are given by :

$$\frac{d\sigma_{\chi e}}{dT_\chi} = \bar{\sigma}_{e\chi} \frac{m_e^2 m_\chi^2}{\mu_{e\chi}^2} \frac{F_{\text{DM}}^2(q^2)}{s_{\text{CR}} T_\chi^{\text{max}}} \quad (13)$$

and,

$$\frac{d\sigma_{\chi e}}{dE_R} = \bar{\sigma}_{e\chi} \frac{m_e^2 m_\chi^2}{\mu_{e\chi}^2} \frac{F_{\text{rec}}^2(q^2)}{s_\chi E_R^{\text{max}}} \quad (14)$$

The differential recoil rate of electrons in SUPER-K can be calculated to be

$$\frac{dR}{dE_R} = \aleph \int_{T_\chi^{\text{min}}(E_R)}^{\infty} dT_\chi \left(\frac{d\Phi_\chi}{dT_\chi} \right)_e \frac{d\sigma_{\chi e}}{dE_R} \quad (15)$$

where the factor \aleph takes into account the number density of the target electrons in the detector, E_R is the recoil energy and T_χ^{min} is the minimum DM energy required to produce a recoil of E_R in the detector, given by

$$T_\chi^{\text{min}} = \left(\frac{E_R}{2} - m_\chi \right) \left[1 \pm \sqrt{1 + \frac{2E_R}{m_e} \frac{(m_e + m_\chi)^2}{(2m_\chi - E_R)^2}} \right] \quad (16)$$

with + and - applicable for $E_R > 2m_\chi$ and $E_R < 2m_\chi$ respectively.

The detection mechanism for XENONnT detector consists of an ionisation process. In the XENONnT detector, an incident DM particle can ionize an electron in the (n, l) shell of a Xenon atom (A). The rate of the ionization process $\chi + A \rightarrow \chi + A^+ + e^-$ is given by

$$\frac{dR_{\text{ion}}}{d \ln E_R} = \tilde{\aleph} \phi_{\text{halo}} \sum_{nl} \frac{d\langle \sigma_{\text{ion}}^{nl} v \rangle}{d \ln E_R} \quad (17)$$

where $\tilde{\aleph}$ is the number of target atoms in the detector, $\phi_{\text{halo}} = n_\chi \bar{v}_\chi$ is the background galactic DM halo flux, and $\frac{d\langle \sigma_{\text{ion}}^{nl} v \rangle}{d \ln E_R}$ is the velocity-averaged differential cross section, given by [43, 44] :

$$\frac{d\langle \sigma_{\text{ion}}^{nl} v \rangle}{d \ln E_R} = \frac{\bar{\sigma}_{e\chi}}{8\mu_{\chi e}^2} \int |F_{\text{rec}}(q)|^2 |f_{\text{ion}}^{nl}(k', q)|^2 \eta(E_\chi^{\text{min}}) q dq, \quad (18)$$

Here F_{rec} is a form factor defined and discussed below (See Eqns. 12, 14), $f_{\text{ion}}^{nl}(k', q)$ is the ionization form factor and q is the momentum transferred (See Appendix A for more details). The mean inverse speed function $\eta(E_\chi^{\text{min}})$ is given by [45]

$$\eta(E_\chi^{\text{min}}) = \int_{E_\chi^{\text{min}}} dE_\chi \phi_{\text{halo}}^{-1} \frac{m_\chi^2}{pE_\chi} \frac{d\phi_\chi}{dT_\chi} \quad (19)$$

where E_χ^{min} refers to the minimum energy that a DM particle must possess to elicit the detector recoil E_R .

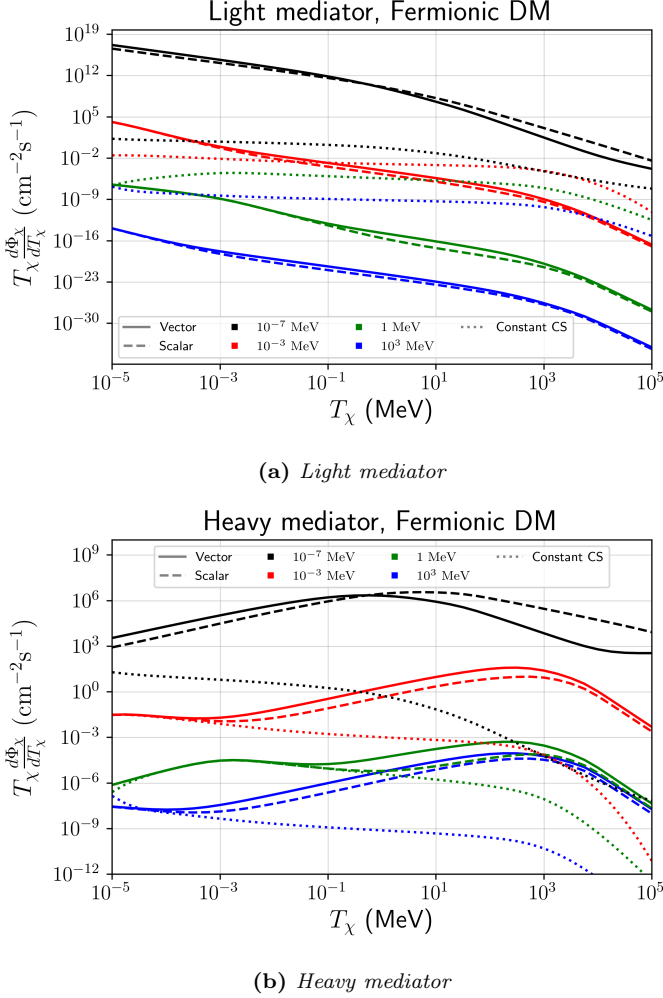


FIG. 1: Plots showing the effect of Lorentz structure of the operators compared with the constant cross-section ($\bar{\sigma}_{e\chi} = 10^{-30} \text{cm}^2$) case, on boosted DM flux. For each case, we plot lines for four DM masses, $m_\chi = 10^{-7}, 10^{-3}, 1, 10^3$ MeV. For the light mediator (Fig. 1a), the modified flux is raised above the constant cross-section case for very light DM masses, while it falls below that for higher masses. However, for the heavy mediator (Fig. 1b) case, the modified flux is higher than the constant cross-section case for all DM masses.

Note that $E_\chi^{\min} = T_\chi^{\min} + m_\chi$. Also note that this convolution need not be done for SUPER-K.

The effect of the energy dependence on DM flux can be understood from Fig. 1. The minimum energy the DM particles must possess, in order to impart a detectable recoil to the target electrons, sets the lower limit (T_χ^{\min}) of the relevant DM energy range. Very high DM energies ($T_\chi > 10^3$ MeV) are not relevant, since the differential flux ($d\Phi_\chi/dT_\chi$) falls off at high DM energies.

For heavy mediators (vector and scalar), the boost is more effective in increasing the flux at high DM energies when energy dependence of cross section is taken care of. This is applicable for all DM masses, hence it is expected that including energy dependence for heavy me-

diator will improve the bounds as compared to the constant cross section scenario. For light mediators (vector and scalar), the energy dependent boost is less effective than constant cross section scenario for higher DM masses. This allows us to predict that the light mediator bounds will be stronger than the energy independent bounds for lighter DM, but the same will become weaker for heavier DM. Also, since in the T_χ regime relevant to us, the vector mediator boosted DM flux is greater than the scalar case, we can expect exclusion bounds to be stronger for the former. Finally, since the flux falls for heavier DM, we expect exclusion bounds to be stronger for lighter DM. We find, in Section IV, that the exclusion bounds we obtain follow these trends.

III. SIMPLIFIED MODEL AND EFFECTIVE OPERATORS

Without referring to an underlying model, we consider a fermionic DM particle χ of mass m_χ , which couples to electrons only. This type of scenario can arise in several leptophilic models of particle DM [46–55]. For concreteness, we assume this interaction is mediated by a scalar (ϕ) or a vector mediator (B_μ).

$$\mathcal{L} = g_{\chi\phi}\phi\bar{\chi}\chi + g_{e\phi}\phi\bar{e}e \quad \text{or} \quad (20)$$

$$= g_{\chi A'} A'_\mu \bar{\chi}\gamma^\mu\chi + g_{e A'} A'_\mu \bar{e}\gamma^\mu e \quad (21)$$

Depending on the type of operator, we expect the differential rates to change. In this section, we inspect the effect of the Lorentz structure on $F_{\text{DM}}^2(q^2)$ and on the differential rate.

A. Scalar Mediator

Considering a scalar mediator (denoted as ϕ), one can calculate F_{DM}^2 for the interaction between CRE and non-relativistic DM, using Eqn. 12 to obtain

$$F_{\text{DM}}^2(q) = \frac{(q_{\text{ref}}^2 - m_\phi^2)^2}{(q^2 - m_\phi^2)^2} \frac{(2m_\chi + T_\chi)(2m_e^2 + m_\chi T_\chi)}{4m_\chi m_e^2} \quad (22)$$

The differential cross section ($d\sigma/dT_\chi$) w.r.t. the DM energy (T_χ), is :

$$\frac{d\sigma_{\chi e}}{dT_\chi} = \bar{\sigma}_{e\chi} \frac{(q_{\text{ref}}^2 - m_\phi^2)^2}{(q^2 - m_\phi^2)^2} \left\{ \frac{m_\chi}{4\mu_{e\chi}^2} \frac{(2m_\chi + T_\chi)(2m_e^2 + m_\chi T_\chi)}{s_{\text{CR}} T_\chi^{\max}} \right\} \quad (23)$$

The form factor F_{rec} and the differential cross-section w.r.t. the recoil energy of the detector ($d\sigma_{\chi e}/dE_R$) are obtained from Eqn. (22) and Eqn. (23) by performing the substitutions prescribed in the previous section, viz. $m_e \leftrightarrow m_\chi, T_\chi \rightarrow E_R, T_e \rightarrow T_\chi, s_{\text{CR}} \rightarrow s_\chi$.

B. Vector Mediator

Using a similar treatment for the vector mediator (denoted by A'), we find that

$$F_{\text{DM}}^2(q^2) = \frac{(q_{\text{ref}}^2 - m_{A'}^2)^2}{(q^2 - m_{A'}^2)^2} \frac{1}{2m_\chi m_e^2} \left(2m_\chi (m_e + T_e)^2 - T_\chi \left\{ (m_e + m_\chi)^2 + 2m_\chi T_e \right\} + m_\chi T_\chi^2 \right) \quad (24)$$

and,

$$\frac{d\sigma_{\chi e}}{dT_\chi} = \bar{\sigma}_{e\chi} \frac{(q_{\text{ref}}^2 - m_{A'}^2)^2}{(q^2 - m_{A'}^2)^2} \frac{m_\chi}{2\mu_{e\chi}^2 s_{\text{CR}} T_\chi^{\text{max}}} \left\{ 2m_\chi (m_e + T_e)^2 - T_\chi \left\{ (m_e + m_\chi)^2 + 2m_\chi T_e \right\} + m_\chi T_\chi^2 \right\} \quad (25)$$

IV. RESULTS

In this section, we performed a χ^2 analysis to obtain novel limits using XENONnT (a low energy threshold recoil experiment) and SUPER-K (a high energy threshold recoil experiment) data.

The exclusion region is obtained using the following definitions for χ^2 :

$$\chi^2 = \sum_i \frac{(O_i - E_i)^2}{(\sigma_i)_{\text{data}}^2} \quad (26)$$

$$\Delta\chi^2 = \chi^2(\text{BDM} + B_0) - \chi^2(B_0 \text{ only}) \quad (27)$$

where, O_i are the observed number of events, E_i are the expected number of events and $(\sigma_i)_{\text{data}}$ is uncertainty in the measured data, for the i^{th} recoil energy bin. For the (BDM + B_0) case, to calculate the E_i values, we sum the BDM signal and the background B_0 for each energy bin. Clearly, if the BDM contribution explains experimental data, $\Delta\chi^2$ must be less than 0 corresponding with a better fit.

The XENON1T collaboration had reported a 3.5σ excess of events in the electron recoil range of $1 \text{ keV} < E_{\text{R}} < 7 \text{ keV}$ [6]. However, a recent dataset from the XENONnT experiment [7], aimed at verifying the aforementioned excess, shows that no such excess exists. We use the data from this experiment for our analysis. To derive the exclusion limit with the 95% confidence, we demand $\Delta\chi^2 > 40.1$ that corresponds to 27 degrees of freedom.

For SUPER-K, we use the SK-I data which was taken for total 1497 days of live-time [56]. The detector originally looked for the Diffuse Supernovae Background events via inverse beta decay $\bar{\nu}_e + p \rightarrow n + e^+$. In the present work, we assume that the observed events are consistent with the background and hence the signal due to DM should be consistent with the data within the uncertainty. Since an estimate of the background is not found in the literature for SK-I data, we take $\chi^2(B_0 \text{ only})|_{\text{SK}} = 0$. The excluded region satisfies $\Delta\chi^2 > 26.3$ which corresponds to 95% exclusion limit for 16 degrees of freedom.

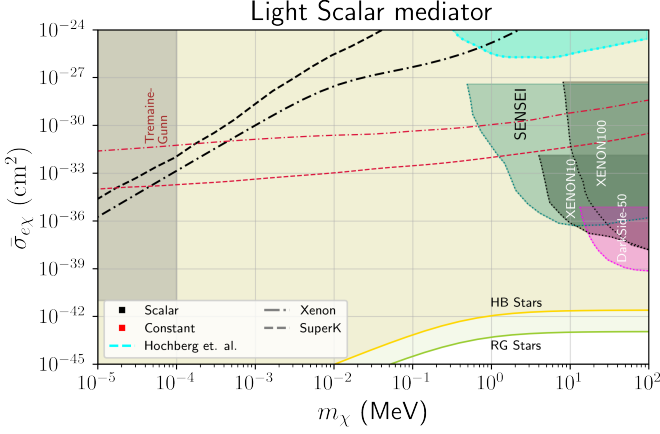
Both SUPER-K and XENONnT experiments are located deep underground to reduce background, but this also attenuates the DM flux entering the detector. The attenuation of DM particles happens mainly due to the interaction with electrons in the Earth's surface, significantly altering the DM flux reaching the detector. While a detailed study of the effects of attenuation on boosted DM is beyond the scope of this paper, we have determined the attenuation bound considering a DM particle with $T_\chi = 1 \text{ GeV}$. This attenuation bound corresponds to the cross section for which the DM particle (with $T_\chi = 1 \text{ GeV}$) can impart the threshold recoil energy in the detector. For this, we solve the following equation to calculate the energy T_r lost by the dark matter

$$\frac{dT_\chi}{dx} = - \sum_T n_T \int_0^{T_r^{\text{max}}} \frac{d\sigma}{dT_r} T_r dT_r \quad (28)$$

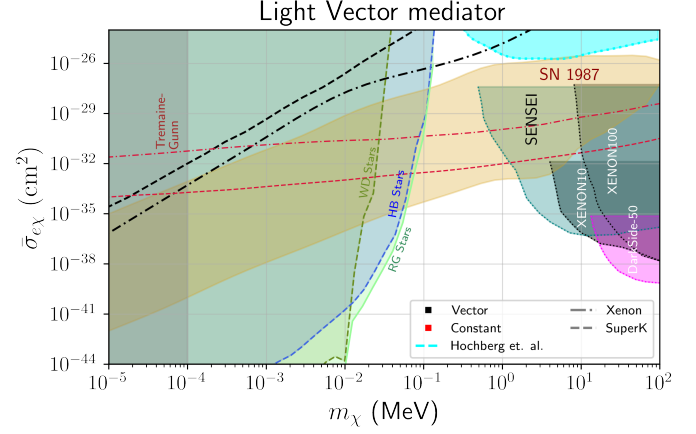
and estimate $\bar{\sigma}_{e\chi}$ so that kinetic energy of the DM particle at depth z , denoted by T_χ^z , is the detector threshold E_{th} , for an initial kinetic energy $T_{\chi,\text{in}} = 1 \text{ GeV}$. The area bounded by the attenuation bound and the exclusion bound is ruled out by our analysis. Also note that ionisation effects could dominate above $T_\chi = 1 \text{ GeV}$. Moreover, light DM particles ($m_\chi < m_e$) may backscatter into the atmosphere. In this work, though, we limit ourselves to elastic scattering, leaving a more elaborate treatment for future work. Note that the attenuation limits exist only for the heavy mediators. There is no attenuation bound shown for the light mediator scenario with elastic scatterings and the attenuation bound shown for heavy mediator may also vary once the effects mentioned above are taken into account.

The exclusion bounds arising from XENONnT and SUPER-K data are shown in Fig. 2, 3 in the heavy and light mediator regime for scalar and vector operators. We find that SUPER-K sets the stronger bound for heavy scalar and vector mediators. For light mediators, it is XENONnT that sets the stronger bound, even though SUPER-K has a greater live-time and a larger effective target density \aleph . Fermionic DM lighter than $\mathcal{O}(100 \text{ eV})$ is highly constrained by the Tremaine-Gunn bound [63–66]⁴. We find that, for the light mediator case, the energy dependent cross section bounds are stronger than the constant cross section bounds for keV-scale DM, and weaker for heavier DM. For the heavy mediator case, the energy-dependent bound is stronger than the constant cross-section case and competitive for heavier DM. This is, as previously discussed in Section II, a consequence of BDM flux behaviour, shown in Fig. 1. Ofcourse, the exact value of DM mass at which energy independent cross section bounds take over as m_χ is increased cannot be predicted by the flux plots alone, since there is T_χ

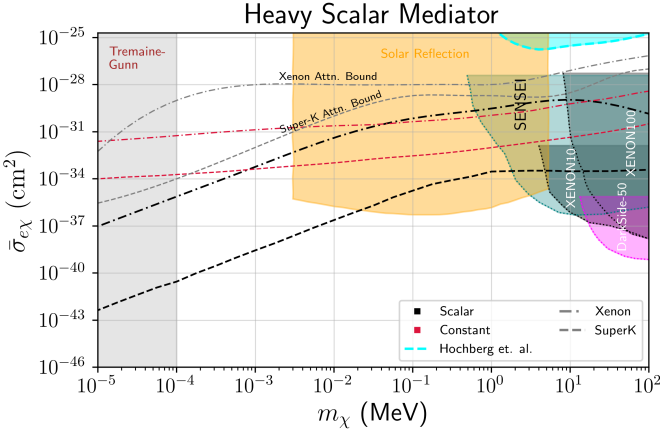
⁴ For a possible way to evade this bound, see Ref. [67]



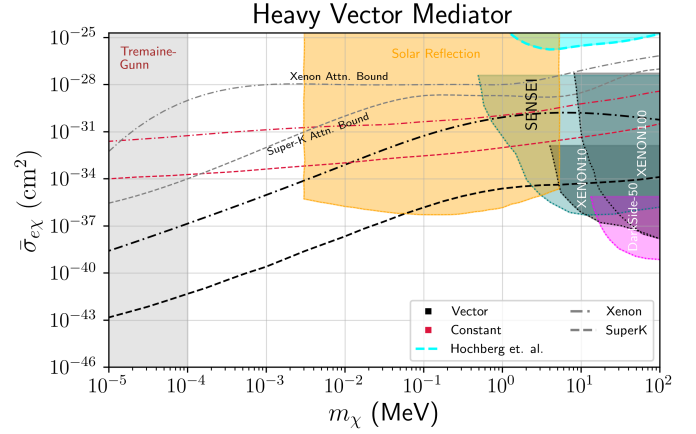
(a) Light Scalar mediator



(a) Light Vector mediator



(b) Heavy Scalar mediator



(b) Heavy Vector mediator

FIG. 2: Exclusion bounds on the cross-section is shown as a function of the DM mass for the scalar mediator. Exclusion bound for constant cross-section scenario is also plotted (in red). For each of these scenarios, the results are shown for two different experiments - XENONnT and SUPER-K, differentiated by the linestyles used in the plot. The direct detection bounds from XENON10, XENON100, SENSEI [57–59] and DARKSIDE-50 [60] are also plotted. The grey shaded region represents the region excluded due to the Tremeine-Gunn bound. The bound arising due to DM attenuation is also given for heavy mediator scenario. Note that the region between attenuation bound and exclusion bound is ruled out. Bounds from stellar cooling constraints [61] are also shown for light mediator case, while for the heavy mediator case, the bound from solar reflection of DM [30, 45] is shown.

FIG. 3: Exclusion bounds on the cross-section is shown as a function of the DM mass for the vector mediator. Exclusion bound for constant cross-section scenario is also plotted (in red). For each of these scenarios, the results are shown for two different experiments - XENONnT and SUPER-K, differentiated by the linestyles used in the plot. The direct detection bounds from XENON10, XENON100, SENSEI [57–59] and DARKSIDE-50 [60] are also plotted. The grey shaded region represents the region excluded due to the Tremeine-Gunn bound. The bound arising due to DM attenuation is also given for heavy mediator scenario. Bounds from stellar and supernovae (SN 1987) cooling [61, 62] are also shown for light mediator case. Constraint due to solar reflection of DM, relevant for the heavy mediator case [30, 45], is shown in amber color.

dependence in differential cross section relevant at the detector end as well. As discussed in Section II, the vector mediator case yields slightly stronger bounds than the scalar mediator case. We also plot the DM attenuation bound for XENONnT and SUPER-K, for heavy mediator scenario.

Similar results have been obtained for vector mediator in Ref. [30], but it should be noted that the dataset

used in Ref. [30] is based on XENON100 and XENON1T’s S2-only analysis [68, 69], while we use the data based on XENONnT’s S1-S2 analysis and thus the exclusion bounds we provide are slightly different from those obtained in Ref. [30].

Our bounds for boosted DM can also be compared to bounds obtained for non-relativistic DM using novel materials with extremely low recoil trigger. A prototype device that can measure single photons made using Su-

perconducting Nanowires is described in Refs. [70, 71]. The best bounds obtained from the device is also shown. The bounds they obtained are competitive with our bounds for DM masses $m_\chi \gtrsim \mathcal{O}(1 \text{ MeV})$. At the moment our bounds are much stronger for lower masses, but proposed devices with materials like NbN and Al might give better exclusions in the near future.

We have included constraints arising from astrophysical sources like Red Giant and Horizontal Branch stars [61] for light mediators. For light scalar mediators, stellar cooling bounds are so severe that they rule out the whole region constrained in this work. In case of a vector mediator, bounds are mild for ultra-light mediator due to in-medium effects [72, 73]. Bounds from solar reflection of DM [30, 45] are important in the heavy mediator case. The cosmological constraints from Big Bang Nucleosynthesis (BBN) rule out thermal DM of $m_\chi \lesssim 10 \text{ MeV}$ stringently [73, 74]. Similarly, the CMB observations constrain DM annihilating to an e^-e^+ pair severely [75]. However, BBN bounds are relaxed in models where DM couples to both neutrinos and electrons [76]. Also, if there is an elaborate dark sector associated in these models so that DM mostly annihilate to other dark sector particles, BBN and CMB constraints can be relaxed even further [77]. For the heavy mediator case, some of the proposed or approved future experimental facilities and detection strategies, discussed in Ref. [78], have great potential to explore the parameter space probed by XENONnT and SUPER-K shown in Fig. 2 and Fig. 3.

V. SUMMARY & OUTLOOK

Dark Matter (DM) poses a unique challenge in physics at the moment. On one hand, a lot of cosmological evidence points to its existence, but, on the other hand, its particle nature is completely unknown. Detection of DM has primarily relied on large terrestrial experiments with a lot of targets for a DM particle from the Milky Way galactic halo to impinge on. These direct detection experiments can then measure the recoil of the target and thus measure both the kinetic energy and mass of the DM particle.

The challenge to this strategy comes from the fact that DM in our galactic halo is non-relativistic, with $v \approx 10^{-3} c$. With detector recoil triggers being $\sim \mathcal{O}(\text{keV})$ or larger, the mass of the DM that can be detected is $\sim \mathcal{O}(\text{MeV})$. In order to detect low mass DM particles, we can take any of the following measures. The obvious one is to lower the detector recoil trigger. This involves finding new detector materials and building new detectors. A lot of work has been undertaken on this front, notably the use of Superconducting Nanowires to build a device with the threshold energy of $\sim \mathcal{O}(\text{eV})$ [70, 71]. We, however, focus on a strategy that allows us to use existing detector data to put exclusion limits on low mass DM, viz. by boosting DM particles in the galactic halo using cosmic ray electrons to relativistic speeds, so

that even very low mass DM particles can trigger the detector.

In this paper, we considered the effect of such a boost as well as the effect of the Lorentz structure of the couplings, which has been missing in most of the literature till now. DM particles can interact with SM electrons via a ‘dark’ mediator, which is charged under both the DM gauge group and the SM electroweak gauge group. We considered mediators of two kinds - vector and scalar. For each of the cases, we explored the effect when the mediator is very heavy or when the mediator is very light, using data from XENONnT and SUPER-KAMIOKANDE (SUPER-K).

Boosts due to cosmic ray electrons drastically change the DM flux as seen on Earth. The effect though is quite different for different DM masses as well as for different mediator masses. For light mediators, the boosted flux is suppressed below the constant cross-section flux for relatively heavier DM masses, while it is raised above that level for light DM masses. This is very different for heavy mediators, for which the DM flux is augmented above the constant cross-section case for all masses. This behaviour is largely independent of the nature of the mediator, though there are some numerical differences in the scalar and vector cases. This behaviour, in turn, leads us to expect that the energy dependence of the cross-section can provide stronger bounds for lighter DM in the light mediator case, while providing stronger bounds for a large range of DM masses in the heavy mediator case. Our analysis meets this expectation.

The two experiments whose dataset we use differ in two fundamental aspects. While SUPER-K has a much larger number of target electrons (as can be seen by the different values of \aleph used in our analysis), XENONnT has a much smaller trigger energy. The live-time for the dataset from SUPER-K is also longer than for the dataset from XENONnT. We find that for the light mediator case, XENONnT gives stronger bounds on both the cross-section and the electron-mediator couplings compared to SUPER-K, while for the heavy mediator case, the reverse is true.

The exclusion bounds on the cross-section obtained from our analysis, for the light mediator case, is competitive with that obtained by the authors of Refs. [70, 71] using their prototype superconducting nanowire single photon detector (SNSPD) to detect non-relativistic DM particles for masses above $\sim 1 \text{ MeV}$. Our bounds extend much further in the lower mass regions, however, and are also stronger in the heavy mediator case. Of course, the projected limits using novel materials like NbN and Al are much stronger than their current observed limits or ours.

In the analysis presented here, we tried to calculate the effect of both, boosts for DM particles and the Lorentz structure of the operators involved. We find that both effects modify the bounds from the existing constant cross-section case. We also perform a preliminary investigation of the attenuation of DM particles. A more rigorous analysis is in progress and will be pre-

sented in a future work.

ACKNOWLEDGEMENTS

D.G. acknowledges support through the Ramanujan Fellowship and MATRICS Grant of the Department of Science and Technology, Government of India. D.B. acknowledges financial support through the National Postdoctoral Fellowship (NPDF), SERB,

PDF/2021/002206. Work of A.G. is supported by the National Research Foundation of Korea (NRF-2019R1C1C1005073). D.S. has received funding from the European Union's Horizon 2020 research and innovation programme under grant agreement No 101002846, ERC CoG "CosmoChart". The authors also thank Arka Banerjee and Susmita Adhikari for their valuable comments on the Tremaine-Gunn bound. We also thank Robert McGehee for his valuable comments on the pre-print.

Appendix A: The Ionization Form Factor

The cross section for the scattering process $\chi(p) + e(k) \rightarrow \chi(p') + e(k')$ is given by

$$d\sigma = \frac{|\mathcal{M}|^2}{v_{\chi e}} \frac{1}{64\pi^2 E_\chi E'_\chi E_e E'_e} \frac{1}{(2\pi)^3} \delta(\Delta E_\chi - \Delta E_e) f_{i \rightarrow k'}(\vec{q}) d^3\vec{q} d^3\vec{k}' \quad (\text{A1})$$

where the atomic form factor $f_{i \rightarrow k'}(\vec{q})$ takes care of the initial and final states of the electron. Eqn. A1 can be recast [30] to take the form of Eqn. 18, with the ionization form factor $f_{\text{ion}}^{nl}(k', q)$ defined as

$$|f_{\text{ion}}^{nl}(k', q)|^2 = \frac{2k'^3}{(2\pi)^3} \sum_{\text{deg}} |f_{i \rightarrow k'}(\vec{q})|^2 \quad (\text{A2})$$

If the initial and final states are free, then this factor reduces to $f_{i \rightarrow k'}(\vec{q}) = (2\pi)^3 \delta^3(\vec{k} - \vec{k}' + \vec{q})$, which is the case for SUPER-K. For XENONnT, after ionisation, the electron is a free particle, while for the initial state, the contributing electronic orbitals of Xenon are $(5p^6, 5s^2, 4d^{10}, 4p^6, 4s^2)$. The momentum of the final state is given by $k' = \sqrt{2m_e E_R}$. The expression for the ionization form factor is given by the following [30, 43]

$$|f_{\text{ion}}^{nl}(k', q)|^2 = \frac{(2l+1)k'^2}{4\pi^3 q} \int_{|k'-q|}^{k'+q} |\chi_{nl}(k)|^2 k dk \quad (\text{A3})$$

where the radial wave function in momentum space $\chi_{nl}(k)$ can be expressed as a linear combination of the Slater-type orbitals [30, 79, 80], which results in the following expression

$$\begin{aligned} \chi_{nl}(k) = & \sum_j C_{nlj} 2^{n_{lj}-l} \left(\frac{2\pi a_0}{Z_{lj}} \right)^{3/2} \left(\frac{ip a_0}{Z_{lj}} \right)^l \frac{\Gamma(n_{lj} + l + 2)}{\Gamma(l + \frac{3}{2}) \sqrt{(2n_{lj})!}} \\ & \times {}_2F_1 \left[\frac{1}{2}(n_{lj} + l + 2), \frac{1}{2}(n_{lj} + l + 3), l + \frac{3}{2}, - \left(\frac{p a_0}{Z_{lj}} \right)^2 \right] \end{aligned} \quad (\text{A4})$$

Here, ${}_2F_1$ denotes the hypergeometric function, a_0 is the Bohr radius, and the coefficients C_{nlj} , Z_{lj} and n_{lj} are taken from Ref. [79].

-
- [1] M. Bauer and T. Plehn, *Yet Another Introduction to Dark Matter: The Particle Physics Approach*, Lecture Notes in Physics, Vol. 959 (Springer, 2019) arXiv:1705.01987 [hep-ph].
 - [2] G. Bertone, D. Hooper, and J. Silk, Particle dark matter: Evidence, candidates and constraints, *Phys. Rept.* **405**, 279 (2005), arXiv:hep-ph/0404175.
 - [3] M. Lisanti, Lectures on Dark Matter Physics, in *Theoretical Advanced Study Institute in Elementary Particle Physics: New Frontiers in Fields and Strings* (2017) pp. 399–446, arXiv:1603.03797 [hep-ph].
 - [4] J. Conrad, Indirect Detection of WIMP Dark Matter: a compact review, in *Interplay between Particle and Astroparticle physics* (2014) arXiv:1411.1925 [hep-ph].

- [5] R. Bernabei *et al.* (DAMA), First results from DAMA/LIBRA and the combined results with DAMA/NaI, *Eur. Phys. J. C* **56**, 333 (2008), arXiv:0804.2741 [astro-ph].
- [6] E. Aprile *et al.* (XENON), Excess electronic recoil events in XENON1T, *Phys. Rev. D* **102**, 072004 (2020), arXiv:2006.09721 [hep-ex].
- [7] E. Aprile *et al.* (XENON), Search for New Physics in Electronic Recoil Data from XENONnT, (2022), arXiv:2207.11330 [hep-ex].
- [8] J. A. Dror, G. Elor, R. McGehee, and T.-T. Yu, Absorption of sub-MeV fermionic dark matter by electron targets, *Phys. Rev. D* **103**, 035001 (2021), [Erratum: *Phys.Rev.D* 105, 119903 (2022)], arXiv:2011.01940 [hep-ph].
- [9] J. A. Dror, G. Elor, and R. McGehee, Directly Detecting Signals from Absorption of Fermionic Dark Matter, *Phys. Rev. Lett.* **124**, 18 (2020), arXiv:1905.12635 [hep-ph].
- [10] J. A. Dror, G. Elor, and R. McGehee, Absorption of Fermionic Dark Matter by Nuclear Targets, *JHEP* **02**, 134, arXiv:1908.10861 [hep-ph].
- [11] T. Bringmann and M. Pospelov, Novel direct detection constraints on light dark matter, *Phys. Rev. Lett.* **122**, 171801 (2019), arXiv:1810.10543 [hep-ph].
- [12] C. V. Cappiello, K. C. Y. Ng, and J. F. Beacom, Reverse Direct Detection: Cosmic Ray Scattering With Light Dark Matter, *Phys. Rev. D* **99**, 063004 (2019), arXiv:1810.07705 [hep-ph].
- [13] C. V. Cappiello and J. F. Beacom, Erratum: Strong new limits on light dark matter from neutrino experiments [*Phys. Rev. D* 100, 103011 (2019)], *Phys. Rev. D* **100**, 103011 (2019), [Erratum: *Phys.Rev.D* 104, 069901 (2021)], arXiv:1906.11283 [hep-ph].
- [14] Y. Ema, F. Sala, and R. Sato, Light Dark Matter at Neutrino Experiments, *Phys. Rev. Lett.* **122**, 181802 (2019), arXiv:1811.00520 [hep-ph].
- [15] J. B. Dent, B. Dutta, J. L. Newstead, I. M. Shoemaker, and N. T. Arellano, Present and future status of light dark matter models from cosmic-ray electron upscattering, *Phys. Rev. D* **103**, 095015 (2021), arXiv:2010.09749 [hep-ph].
- [16] Y. Jho, J.-C. Park, S. C. Park, and P.-Y. Tseng, Leptonic New Force and Cosmic-ray Boosted Dark Matter for the XENON1T Excess, *Phys. Lett. B* **811**, 135863 (2020), arXiv:2006.13910 [hep-ph].
- [17] J. Bramante, B. J. Kavanagh, and N. Raj, Scattering searches for dark matter in subhalos: neutron stars, cosmic rays, and old rocks, (2021), arXiv:2109.04582 [hep-ph].
- [18] Y. Farzan and S. Palomares-Ruiz, Dips in the Diffuse Supernova Neutrino Background, *JCAP* **06**, 014, arXiv:1401.7019 [hep-ph].
- [19] C. A. Argüelles, A. Kheirandish, and A. C. Vincent, Imaging Galactic Dark Matter with High-Energy Cosmic Neutrinos, *Phys. Rev. Lett.* **119**, 201801 (2017), arXiv:1703.00451 [hep-ph].
- [20] W. Yin, Highly-boosted dark matter and cutoff for cosmic-ray neutrinos through neutrino portal, *EPJ Web Conf.* **208**, 04003 (2019), arXiv:1809.08610 [hep-ph].
- [21] Y. Jho, J.-C. Park, S. C. Park, and P.-Y. Tseng, Cosmic-Neutrino-Boosted Dark Matter (ν BDM), (2021), arXiv:2101.11262 [hep-ph].
- [22] A. Das and M. Sen, Boosted dark matter from diffuse supernova neutrinos, (2021), arXiv:2104.00027 [hep-ph].
- [23] D. Ghosh, A. Guha, and D. Sachdeva, Exclusion limits on dark matter-neutrino scattering cross section, *Phys. Rev. D* **105**, 103029 (2022).
- [24] J. B. Dent, B. Dutta, J. L. Newstead, and I. M. Shoemaker, Bounds on Cosmic Ray-Boosted Dark Matter in Simplified Models and its Corresponding Neutrino-Floor, *Phys. Rev. D* **101**, 116007 (2020), arXiv:1907.03782 [hep-ph].
- [25] G. Elor, R. McGehee, and A. Pierce, Maximizing Direct Detection with HYPER Dark Matter, (2021), arXiv:2112.03920 [hep-ph].
- [26] B. Chauhan, B. Dasgupta, and A. Dighe, Large-energy single hits at JUNO from atmospheric neutrinos and dark matter, *Phys. Rev. D* **105**, 095035 (2022), arXiv:2111.14586 [hep-ph].
- [27] J.-W. Wang, A. Granelli, and P. Ullio, Direct Detection Constraints on Blazar-Boosted Dark Matter, *Phys. Rev. Lett.* **128**, 221104 (2022), arXiv:2111.13644 [astro-ph.HE].
- [28] A. Granelli, P. Ullio, and J.-W. Wang, Blazar-boosted dark matter at Super-Kamiokande, *JCAP* **07** (07), 013, arXiv:2202.07598 [astro-ph.HE].
- [29] G. Herrera and A. Ibarra, Direct detection of non-galactic light dark matter, *Phys. Lett. B* **820**, 136551 (2021), arXiv:2104.04445 [hep-ph].
- [30] Q.-H. Cao, R. Ding, and Q.-F. Xiang, Searching for sub-MeV boosted dark matter from xenon electron direct detection, *Chin. Phys. C* **45**, 045002 (2021), arXiv:2006.12767 [hep-ph].
- [31] Y. Ema, F. Sala, and R. Sato, Neutrino experiments probe hadrophilic light dark matter, *SciPost Phys.* **10**, 072 (2021), arXiv:2011.01939 [hep-ph].
- [32] C. Xia, Y.-H. Xu, and Y.-F. Zhou, Azimuthal asymmetry in cosmic-ray boosted dark matter flux, (2022), arXiv:2206.11454 [hep-ph].
- [33] M. J. Boschini *et al.*, HelMod in the works: from direct observations to the local interstellar spectrum of cosmic-ray electrons, *Astrophys. J.* **854**, 94 (2018), arXiv:1801.04059 [astro-ph.HE].
- [34] M. Ackermann *et al.* (Fermi-LAT), Measurement of separate cosmic-ray electron and positron spectra with the Fermi Large Area Telescope, *Phys. Rev. Lett.* **108**, 011103 (2012), arXiv:1109.0521 [astro-ph.HE].
- [35] A. A. Abdo *et al.* (Fermi-LAT), Measurement of the Cosmic Ray e^+ plus e^- spectrum from 20 GeV to 1 TeV with the Fermi Large Area Telescope, *Phys. Rev. Lett.* **102**, 181101 (2009), arXiv:0905.0025 [astro-ph.HE].
- [36] M. Ackermann *et al.* (Fermi-LAT), Fermi LAT observations of cosmic-ray electrons from 7 GeV to 1 TeV, *Phys. Rev. D* **82**, 092004 (2010), arXiv:1008.3999 [astro-ph.HE].

- [37] S. Abdollahi *et al.* (Fermi-LAT), Cosmic-ray electron-positron spectrum from 7 GeV to 2 TeV with the Fermi Large Area Telescope, *Phys. Rev. D* **95**, 082007 (2017), arXiv:1704.07195 [astro-ph.HE].
- [38] M. Aguilar *et al.* (AMS), Precision Measurement of the ($e^+ + e^-$) Flux in Primary Cosmic Rays from 0.5 GeV to 1 TeV with the Alpha Magnetic Spectrometer on the International Space Station, *Phys. Rev. Lett.* **113**, 221102 (2014).
- [39] O. Adriani *et al.* (PAMELA), The cosmic-ray electron flux measured by the PAMELA experiment between 1 and 625 GeV, *Phys. Rev. Lett.* **106**, 201101 (2011), arXiv:1103.2880 [astro-ph.HE].
- [40] O. Adriani *et al.* (CALET), Energy Spectrum of Cosmic-Ray Electron and Positron from 10 GeV to 3 TeV Observed with the Calorimetric Electron Telescope on the International Space Station, *Phys. Rev. Lett.* **119**, 181101 (2017), arXiv:1712.01711 [astro-ph.HE].
- [41] A. C. Cummings, E. C. Stone, B. C. Heikkila, N. Lal, W. R. Webber, G. Jóhannesson, I. V. Moskalenko, E. Orlando, and T. A. Porter, Galactic Cosmic Rays in the Local Interstellar Medium: Voyager 1 Observations and Model Results, *Astrophys. J.* **831**, 18 (2016).
- [42] E. C. Stone, A. C. Cummings, F. B. McDonald, B. C. Heikkila, N. Lal, and W. R. Webber, Voyager 1 Observes Low-Energy Galactic Cosmic Rays in a Region Depleted of Heliospheric Ions, *Science* **341**, 150 (2013).
- [43] R. Essig, J. Mardon, and T. Volansky, Direct Detection of Sub-GeV Dark Matter, *Phys. Rev. D* **85**, 076007 (2012), arXiv:1108.5383 [hep-ph].
- [44] R. Essig, M. Fernandez-Serra, J. Mardon, A. Soto, T. Volansky, and T.-T. Yu, Direct Detection of sub-GeV Dark Matter with Semiconductor Targets, *JHEP* **05**, 046, arXiv:1509.01598 [hep-ph].
- [45] H. An, M. Pospelov, J. Pradler, and A. Ritz, Directly Detecting MeV-scale Dark Matter via Solar Reflection, *Phys. Rev. Lett.* **120**, 141801 (2018), [Erratum: *Phys.Rev.Lett.* 121, 259903 (2018)], arXiv:1708.03642 [hep-ph].
- [46] M. Pospelov, A. Ritz, and M. B. Voloshin, Secluded WIMP Dark Matter, *Phys. Lett. B* **662**, 53 (2008), arXiv:0711.4866 [hep-ph].
- [47] B. Batell, M. Pospelov, and A. Ritz, Exploring Portals to a Hidden Sector Through Fixed Targets, *Phys. Rev. D* **80**, 095024 (2009), arXiv:0906.5614 [hep-ph].
- [48] X. Chu, T. Hambye, and M. H. G. Tytgat, The Four Basic Ways of Creating Dark Matter Through a Portal, *JCAP* **05**, 034, arXiv:1112.0493 [hep-ph].
- [49] A. Alves, S. Profumo, and F. S. Queiroz, The dark Z' portal: direct, indirect and collider searches, *JHEP* **04**, 063, arXiv:1312.5281 [hep-ph].
- [50] E. Izaguirre, G. Krnjaic, P. Schuster, and N. Toro, New Electron Beam-Dump Experiments to Search for MeV to few-GeV Dark Matter, *Phys. Rev. D* **88**, 114015 (2013), arXiv:1307.6554 [hep-ph].
- [51] E. Izaguirre, G. Krnjaic, P. Schuster, and N. Toro, Analyzing the Discovery Potential for Light Dark Matter, *Phys. Rev. Lett.* **115**, 251301 (2015), arXiv:1505.00011 [hep-ph].
- [52] G. Krnjaic, Probing Light Thermal Dark-Matter With a Higgs Portal Mediator, *Phys. Rev. D* **94**, 073009 (2016), arXiv:1512.04119 [hep-ph].
- [53] E. Izaguirre, Y. Kahn, G. Krnjaic, and M. Moschella, Testing Light Dark Matter Coannihilation With Fixed-Target Experiments, *Phys. Rev. D* **96**, 055007 (2017), arXiv:1703.06881 [hep-ph].
- [54] K. Harigaya, R. McGehee, H. Murayama, and K. Schutz, A predictive mirror twin Higgs with small Z_2 breaking, *JHEP* **05**, 155, arXiv:1905.08798 [hep-ph].
- [55] E. Bernreuther, S. Heeba, and F. Kahlhoefer, Resonant sub-GeV Dirac dark matter, *JCAP* **03**, 040, arXiv:2010.14522 [hep-ph].
- [56] K. Bays *et al.* (Super-Kamiokande), Supernova Relic Neutrino Search at Super-Kamiokande, *Phys. Rev. D* **85**, 052007 (2012), arXiv:1111.5031 [hep-ex].
- [57] R. Essig, A. Manalaysay, J. Mardon, P. Sorensen, and T. Volansky, First Direct Detection Limits on sub-GeV Dark Matter from XENON10, *Phys. Rev. Lett.* **109**, 021301 (2012), arXiv:1206.2644 [astro-ph.CO].
- [58] R. Essig, T. Volansky, and T.-T. Yu, New Constraints and Prospects for sub-GeV Dark Matter Scattering off Electrons in Xenon, *Phys. Rev. D* **96**, 043017 (2017), arXiv:1703.00910 [hep-ph].
- [59] L. Barak *et al.* (SENSEI), SENSEI: Direct-Detection Results on sub-GeV Dark Matter from a New Skipper-CCD, *Phys. Rev. Lett.* **125**, 171802 (2020), arXiv:2004.11378 [astro-ph.CO].
- [60] P. Agnes *et al.* (DarkSide-50), Search for dark matter particle interactions with electron final states with DarkSide-50, (2022), arXiv:2207.11968 [hep-ex].
- [61] E. Hardy and R. Lasenby, Stellar cooling bounds on new light particles: plasma mixing effects, *JHEP* **02**, 033, arXiv:1611.05852 [hep-ph].
- [62] J. H. Chang, R. Essig, and S. D. McDermott, Supernova 1987A Constraints on Sub-GeV Dark Sectors, Millicharged Particles, the QCD Axion, and an Axion-like Particle, *JHEP* **09**, 051, arXiv:1803.00993 [hep-ph].
- [63] S. Tremaine and J. E. Gunn, Dynamical role of light neutral leptons in cosmology, *Phys. Rev. Lett.* **42**, 407 (1979).
- [64] C. Di Paolo, F. Nesti, and F. L. Villante, Phase space mass bound for fermionic dark matter from dwarf spheroidal galaxies, *Mon. Not. Roy. Astron. Soc.* **475**, 5385 (2018), arXiv:1704.06644 [astro-ph.GA].
- [65] D. Savchenko and A. Rudakovskiy, New mass bound on fermionic dark matter from a combined analysis of classical dSphs, *Mon. Not. Roy. Astron. Soc.* **487**, 5711 (2019), arXiv:1903.01862 [astro-ph.CO].
- [66] K. Pal, L. V. Sales, and J. Wudka, Ultralight Thomas-Fermi dark matter, *Phys. Rev. D* **100**, 083007 (2019), arXiv:1906.04212 [astro-ph.GA].
- [67] H. Davoudiasl, P. B. Denton, and D. A. McGady, Ultralight fermionic dark matter, *Phys. Rev. D* **103**, 055014 (2021), arXiv:2008.06505 [hep-ph].
- [68] E. Aprile *et al.* (XENON), Low-mass dark matter search using ionization signals in XENON100, *Phys. Rev. D* **94**,

- 092001 (2016), [Erratum: Phys.Rev.D 95, 059901 (2017)], arXiv:1605.06262 [astro-ph.CO].
- [69] E. Aprile *et al.* (XENON), Light Dark Matter Search with Ionization Signals in XENON1T, Phys. Rev. Lett. **123**, 251801 (2019), arXiv:1907.11485 [hep-ex].
- [70] Y. Hochberg, I. Charaev, S.-W. Nam, V. Verma, M. Colangelo, and K. K. Berggren, Detecting Sub-GeV Dark Matter with Superconducting Nanowires, Phys. Rev. Lett. **123**, 151802 (2019), arXiv:1903.05101 [hep-ph].
- [71] Y. Hochberg, B. V. Lehmann, I. Charaev, J. Chiles, M. Colangelo, S. W. Nam, and K. K. Berggren, New Constraints on Dark Matter from Superconducting Nanowires, (2021), arXiv:2110.01586 [hep-ph].
- [72] H. Vogel and J. Redondo, Dark radiation constraints on minicharged particles in models with a hidden photon, JCAP **02**, 029.
- [73] S. Knapen, T. Lin, and K. M. Zurek, Light Dark Matter: Models and Constraints, Phys. Rev. D **96**, 115021 (2017), arXiv:1709.07882 [hep-ph].
- [74] D. Ghosh and D. Sachdeva, Constraints on Axion-Lepton coupling from Big Bang Nucleosynthesis, JCAP **10**, 060, arXiv:2007.01873 [hep-ph].
- [75] N. Aghanim *et al.* (Planck), Planck 2018 results. VI. Cosmological parameters, Astron. Astrophys. **641**, A6 (2020), [Erratum: Astron.Astrophys. 652, C4 (2021)], arXiv:1807.06209 [astro-ph.CO].
- [76] M. Escudero, Neutrino decoupling beyond the Standard Model: CMB constraints on the Dark Matter mass with a fast and precise N_{eff} evaluation, JCAP **02**, 007, arXiv:1812.05605 [hep-ph].
- [77] D. Choudhury, S. Maharana, D. Sachdeva, and V. Sahdev, Dark matter, muon anomalous magnetic moment, and the XENON1T excess, Phys. Rev. D **103**, 015006 (2021), arXiv:2007.08205 [hep-ph].
- [78] B. Batell, N. Blinov, C. Hearty, and R. McGehee, Exploring Dark Sector Portals with High Intensity Experiments, in *2022 Snowmass Summer Study* (2022) arXiv:2207.06905 [hep-ph].
- [79] C. F. Bunge, J. A. Barrientos, and A. V. Bunge, Roothaan-Hartree-Fock Ground-State Atomic Wave Functions: Slater-Type Orbital Expansions and Expectation Values for $Z = 2-54$, Atom. Data Nucl. Data Tabl. **53**, 113 (1993).
- [80] J. Kopp, V. Niro, T. Schwetz, and J. Zupan, DAMA/LIBRA and leptonically interacting Dark Matter, Phys. Rev. D **80**, 083502 (2009), arXiv:0907.3159 [hep-ph].